

DESY 95-028

ISSN 0418-9833

February 1995

Thermodynamics of the Electroweak Phase Transition

W. Buchmüller, Z. Fodor* and A. Hebecker

Deutsches Elektronen-Synchrotron DESY, 22603 Hamburg, Germany

Abstract

We discuss several general aspects of the free energy of the standard model at high temperatures. In particular the Clausius-Clapeyron equation is shown to yield a relation between the latent heat and the jump in the order parameter. The free energy is calculated as function of temperature in resummed perturbation theory to two-loop order. A new resummation procedure is proposed in which the symmetric phase and the Higgs phase are treated differently. A quantitative description of the phase transition is achieved for Higgs masses below ~ 70 GeV. The results are found to be in agreement with recent numerical simulations on large lattices. The phase transition provides no evidence for strong non-perturbative effects in the symmetric phase.

*Address after 1 January 1995: Theory Division, CERN, CH-Geneva 23,
on leave from Institute for Theoretical Physics, Eötvös University, Budapest, Hungary

1 Introduction

In the standard model of electroweak interactions all masses are generated by the Higgs mechanism. At high temperatures this implies, in analogy to superconductivity, a phase transition from a massive low-temperature phase to a massless high-temperature phase, where the electroweak symmetry is “restored” [1]. This transition is of great cosmological importance because baryon-number violating processes fall out of thermal equilibrium below the critical temperature of the phase transition [2]. As a consequence, the present value of the baryon asymmetry of the universe has finally been determined at the electroweak transition.

In recent years quantitative studies of the electroweak phase transition have been carried out by means of resummed perturbation theory [3]-[7] and lattice Monte Carlo simulations [8]-[12]. As a first step towards a treatment of the full standard model, the pure SU(2) Higgs model is usually investigated, neglecting fermion effects and the mixing between photon and neutral vector boson. These can be treated in perturbation theory and do not affect the essential infrared problem. There is general agreement that the phase transition is first-order for Higgs masses m_H below the vector boson mass m_W . At larger Higgs masses lattice results [13], general arguments [14] and non-perturbative solutions of gap equations [15] suggest that the first-order transition changes to a smooth crossover. However, this conjecture still remains to be firmly established.

The goal of the present paper is a quantitative study of the thermodynamics of the transition for Higgs masses below 80 GeV. Our analysis will be based on the gauge invariant “order parameter” $\Phi^\dagger\Phi$ [16] and the corresponding free energy [17]. We shall extend our previous one-loop analysis [18] to two-loop order and discuss the connection with the conventional Landau gauge approach. The comparison between one-loop and two-loop results, and also between different resummation procedures, will allow us to estimate the uncertainty of perturbative predictions for thermodynamic observables.

It is well known that the electroweak phase transition is influenced by non-perturbative effects whose size is governed by the confinement scale of the effective three-dimensional theory which describes the high-temperature limit of the SU(2) Higgs model. These effects are particularly relevant in the symmetric phase, and one may worry to what extent a purely perturbative analysis of the phase transition can yield sensible results at all. However, it is not yet known how important these non-perturbative effects are quantitatively for different Higgs masses. As we shall see, at two-loop order our results depend only logarithmically on the infrared cutoff needed in the symmetric phase.

We shall then compare the perturbative results with recent non-perturbative results obtained by numerical Monte Carlo simulations on large lattices [11]. This will enable us to estimate the size of possible non-perturbative corrections.

The paper is organized as follows. In sect. 2 we shall discuss several general aspects of the free energy and the various effective potentials used in connection with the electroweak phase transition. The description of the transition is based on a gauge invariantly coupled source term. The corresponding gauge invariant free energy can be obtained from the minima of the usual Landau gauge potential.

In sect. 3 a useful relation is derived between the latent heat and the gauge invariant order parameter, which follows from the Clausius-Clapeyron equation by dimensional arguments. This relation is exactly satisfied in perturbation theory, and it holds for the lattice results within the estimated errors.

Sect. 4 deals with the free energy at one-loop. A new resummation procedure is introduced which treats the Higgs phase and the symmetric phase differently, reproducing the numerical results of [18] in a different manner. This also clarifies the connection between the gauge invariant and the usual Landau gauge approach. It is shown that the barrier of the gauge invariant effective potential is given by analytic continuations of the convex potential defined by a Legendre transformation.

In Sect. 5 higher order corrections are obtained using the new resummation method of the previous section. This calculation is an extension of the gauge invariant approach of [18] to the two-loop level. While previous numerical results for phase transition parameters are qualitatively reproduced, the convergence of perturbation theory is improved in the new approach.

Sect. 6 contains a comparison with lattice results, showing quantitative agreement within the statistical and systematic errors. For this the most important zero-temperature renormalization effects have to be included at small Higgs masses.

Conclusions are summarized in sect. 7, and the appendix contains the explicit formulae used in sect. 5.

2 Free energy of the SU(2) Higgs model

The action of the SU(2) Higgs model at finite temperature T reads

$$S_\beta[\Phi, W] = \int_\beta dx \operatorname{Tr} \left[\frac{1}{2} W_{\mu\nu} W_{\mu\nu} + (D_\mu \Phi)^\dagger D_\mu \Phi + \mu \Phi^\dagger \Phi + 2\lambda (\Phi^\dagger \Phi)^2 \right], \quad (1)$$

with

$$\Phi = \frac{1}{2}(\sigma + i\vec{\pi} \cdot \vec{\tau}), \quad D_\mu \Phi = (\partial_\mu - igW_\mu)\Phi, \quad W_\mu = \frac{1}{2}\vec{\tau} \cdot \vec{W}_\mu, \quad (2)$$

$$\int_\beta dx = \int_0^\beta d\tau \int_\Omega d^3x, \quad \beta = \frac{1}{T}. \quad (3)$$

Here \vec{W}_μ is the vector field, σ is the Higgs field, $\vec{\pi}$ is the Goldstone field and $\vec{\tau}$ is the triplet of Pauli matrices. In general, we shall consider the limit of infinite spatial volume Ω . For perturbative calculations gauge fixing and ghost terms have to be added to the action (1).

The free energy density of the system, $W(T, J)$, is given by the partition function, i.e., the trace of the density matrix,

$$\exp(-\beta\Omega W(T, J)) = \mathbf{Tr} \exp \left[-\beta \left(\hat{H} + J \int_\Omega d^3x \hat{\Phi}^\dagger \hat{\Phi} \right) \right], \quad (4)$$

where \hat{H} is the Hamilton operator of the theory, and $\hat{\Phi}$ is the operator describing the Higgs field. We have added a source J , with $\partial_\mu J = 0$, coupled to the spatial average of the gauge invariant composite operator $\hat{\Phi}^\dagger \hat{\Phi}$ (here and below the trace operator acting on $\hat{\Phi}^\dagger \hat{\Phi}$ is omitted for brevity). Similarly, one may define a free energy for spatially varying sources $J(x)$. The partition function can be expressed as a euclidian functional integral [19],

$$\exp(-\beta\Omega W(T, J)) = \int_\beta D\Phi D\Phi^\dagger DW_\mu \exp \left(- \int_\beta dx (L + J\Phi^\dagger \Phi) \right), \quad (5)$$

where L is the euclidean lagrangian density, and the bosonic fields Φ and W_μ satisfy periodic boundary conditions at $\tau = 0$ and $\tau = \beta$. Eq. (5) is the starting point of perturbative as well as numerical evaluations of the free energy.

Note, that the source J in eq. (5) couples to a gauge invariant composite field. Hence, the free energy $W(T, J)$ is gauge independent. The spatially constant source J simply redefines the mass term in the action (1). This is in contrast to the usually considered generating function of connected Green functions at zero momentum,

$$\exp(-\beta\Omega \tilde{W}(T, j; J)) = \int_\beta D\Phi D\Phi^\dagger DW_\mu \exp \left(- \int_\beta dx (L + J\Phi^\dagger \Phi + j\sigma) \right). \quad (6)$$

Here the source j couples to a gauge dependent quantity, the field σ . Consequently, $\tilde{W}(T, j; J)$ is gauge dependent and not a physical observable. For later use we have also kept the dependence on the source J .

The generating function $\tilde{W}(T, j; 0)$ can be made finite in the usual way by a multiplicative renormalization of couplings and fields. This is not the case for the free energy

$W(T, J)$, since J couples to a composite field. It is known [20] that two more counter terms, linear and quadratic in J , are necessary in order to subtract the additional divergencies. Hence, the renormalized free energy $W(T, J)$ contains two arbitrary constants in addition to the usual renormalized parameters at zero temperature.

From the free energy $W(T, J)$ a gauge invariant effective potential $V(T, \rho)$ can be obtained as usual by means of a Legendre transformation,

$$V(T, \rho) = W(T, J) - \frac{1}{2}\rho J , \quad (7)$$

where

$$\frac{1}{2}\rho \equiv \frac{1}{\Omega} \int_{\Omega} d^3x \langle \hat{\Phi}^\dagger(x) \hat{\Phi}(x) \rangle = \frac{\partial}{\partial J} W(T, J) \quad (8)$$

is the spatial average of the thermal expectation value of $\hat{\Phi}^\dagger \hat{\Phi}$, which plays the role of an “order parameter” in the SU(2) Higgs model. By definition, the effective potential $V(T, \rho)$ is convex. The ground state of the theory corresponds to a stationary point of the effective potential, where $\partial V(T, \rho)/\partial \rho$ vanishes. In the case of a first-order phase transition two stationary points connected by a straight line (see fig. 3 in sect. 4) represent two coexisting phases.

What is the effect of the ambiguity of the renormalized free energy $W(T, J)$ on the effective potential? Consider two definitions of the free energy, related by

$$\bar{W}(T, J) = W(T, J) + bJ + cJ^2 . \quad (9)$$

The two corresponding effective potentials are $V(T, \rho)$ and

$$\bar{V}(T, \bar{\rho}) = \bar{W}(T, J) - \frac{1}{2}\bar{\rho}J , \quad (10)$$

with

$$\frac{1}{2}\bar{\rho} = \frac{\partial}{\partial J} \bar{W}(T, J) = \frac{1}{2}\rho + b + 2cJ . \quad (11)$$

For stationary points ρ_0 and $\bar{\rho}_0$ of the effective potentials, where

$$\frac{\partial}{\partial \rho} V(T, \rho) |_{\rho=\rho_0} = 0 , \quad \frac{\partial}{\partial \bar{\rho}} \bar{V}(T, \bar{\rho}) |_{\bar{\rho}=\bar{\rho}_0} = 0 , \quad (12)$$

one easily verifies

$$\bar{\rho}_0 = \rho_0 + 2b , \quad \bar{V}(T, \bar{\rho}_0) = V(T, \rho_0) . \quad (13)$$

This means that the free energy of the ground state is independent of the two parameters b and c , whereas the expectation value ρ is arbitrary. However, in the case of more than one stationary point, which is relevant for first-order phase transitions, the difference $\Delta\rho$

between two stationary points is independent of b and c . This difference is a physical observable. Other properties of the gauge invariant potential $V(T, \rho)$, such as the curvature at a local minimum, will in general depend on the parameters b and c .

The functional integral for the free energy may be written as

$$\exp(-\beta\Omega W(T, J)) = 2\pi^2 \int \varphi^3 d\varphi \int_{\beta} D\Phi D\Phi^\dagger DW_\mu \delta\left(\varphi - \frac{1}{\beta\Omega} \int_{\beta} dx \sigma\right) \delta^3\left(\frac{1}{\beta\Omega} \int_{\beta} dx \vec{\pi}\right) \exp\left(-\int_{\beta} dx (L + J\Phi^\dagger\Phi)\right). \quad (14)$$

Here the integrand of the ordinary integral over φ is the exponential of the well known constraint effective potential [21, 22],

$$\exp(-\beta\Omega U(T, \varphi; J)) = \int_{\beta} D\Phi D\Phi^\dagger DW_\mu \delta\left(\varphi - \frac{1}{\beta\Omega} \int_{\beta} dx \sigma\right) \delta^3\left(\frac{1}{\beta\Omega} \int_{\beta} dx \vec{\pi}\right) \exp\left(-\int_{\beta} dx (L + J\Phi^\dagger\Phi)\right). \quad (15)$$

In the infinite volume limit the constraint effective potential $U(T, \varphi; J)$ coincides with the effective potential $\tilde{V}(T, \varphi; J)$. From eqs. (14),(15) one obtains for the free energy,

$$\exp(-\beta\Omega W(T, J)) = 2\pi^2 \int \varphi^3 d\varphi \exp\left(-\beta\Omega \tilde{V}(T, \varphi; J)\right). \quad (16)$$

In the infinite volume limit, this yields

$$W(T, J) = \tilde{V}(T, \varphi_{min}(T, J), J), \quad (17)$$

where $\varphi_{min}(T, J)$ is the global minimum of the effective potential $\tilde{V}(T, \varphi; J)$. For arbitrary values of φ the potential \tilde{V} is gauge dependent. However, its value at the minimum is known to be gauge independent [23], yielding a gauge independent free energy $W(T, J)$.

At the critical temperature T_c of a first-order transition the order parameter ρ and the energy density $E(T, 0)$,

$$E(T, J) = W(T, J) - T \frac{\partial}{\partial T} W(T, J), \quad (18)$$

are discontinuous. The jump in the energy density is the latent heat ΔQ . This discontinuity in ρ and E requires a free energy $W(T, J)$ with the following properties: $W(T, 0)$ must be continuous but not differentiable at $T = T_c$, and the same must hold for $W(T_c, J)$ at $J = 0$. In the following sections we shall verify these features based on a perturbative evaluation of the free energy.

3 Clausius-Clapeyron equation

For the first-order phase transition from liquid to vapour there exists a well known relation between the latent heat and the change of the molar volume, the Clausius-Clapeyron equation [24]. In the electroweak phase transition the “order parameter” $\Phi^\dagger\Phi$ plays the role of the molar volume and a completely analogous relation can be derived.

The electroweak plasma can exist in two phases, the massive low-temperature Higgs phase with free energy $W_b(T, J)$ and the massless high-temperature symmetric phase with free energy $W_s(T, J)$. In the $J - T$ -plane the boundary between the two phases is determined by the equilibrium condition

$$W_s(T, J(T)) = W_b(T, J(T)) , \quad (19)$$

which implies

$$\frac{\partial}{\partial T} (W_s - W_b) = -\frac{\partial}{\partial J} (W_s - W_b) \frac{dJ(T)}{dT} . \quad (20)$$

Using the definitions for latent heat and jump in the order parameter,

$$\frac{\partial}{\partial T} (W_s - W_b) = -\frac{1}{T}\Delta Q \quad , \quad \frac{\partial}{\partial J} (W_s - W_b) = \frac{1}{2}\Delta\rho , \quad (21)$$

one obtains

$$\Delta Q = \frac{1}{2}\Delta\rho T \frac{dJ}{dT} . \quad (22)$$

This is the Clausius-Clapeyron equation of the electroweak phase transition.

So far, we have only used the continuity of the free energy along the phase boundary in the case of a first-order transition. We can now employ the fact that the mass term $\mu + J$ is the only dimensionful parameter of the SU(2) Higgs model. This implies

$$\mu + J(T) = C(g^2, \lambda)T^2 , \quad (23)$$

and therefore

$$T \frac{dJ(T)}{dT} \Big|_{J=0} = 2\mu . \quad (24)$$

To leading order in the couplings one has (cf. (34)), $C(g^2, \lambda) = -(\frac{3}{16}g^2 + \frac{1}{2}\lambda)$. Inserting eq. (24) into eq. (22) we finally obtain¹

$$\Delta Q = -\frac{1}{2}m_H^2\Delta\rho(1 + \mathcal{O}(g^2, \lambda)) . \quad (25)$$

The higher order corrections are due to the difference between the mass parameter $\sqrt{-2\mu}$ and the physical Higgs mass. In the following sections this relation will provide a very useful check on our results.

¹The same result has been derived in a recent paper by Farakos et al. [25] based on renormalization group equations for the effective three-dimensional theory.

4 Free energy in perturbation theory

Near the ground state, $J = 0$, the free energy $W(T, J)$ can be evaluated as power series in the couplings g and λ by means of resummed perturbation theory². Here thermal corrections are added to the tree-level masses of the scalar fields and the longitudinal component of the vector boson field,

$$\delta S_\beta = \beta \int d^3x \left(\frac{1}{2} \alpha_{01} T^2 (\sigma^2 + \pi^2) + \frac{1}{2} \alpha_1 T^2 W_L^2 \right) . \quad (26)$$

The sum of tree-level masses and thermal corrections then enters the boson propagators in loop diagrams, and $\delta S_\beta^c = -\delta S_\beta$ is treated as counter term. In eq. (26) the fields σ and π do not depend on the imaginary time τ . Following Arnold and Espinosa [4], we only resum the static modes of scalar and vector fields. Clearly, this is sufficient to avoid infrared singular contributions from these fields since non-static modes have thermal masses $\mathcal{O}(T)$. For the usual resummation with one-loop thermal counter terms $\sim T^2$ the resummation of static modes is known to be equivalent to the resummation of all modes. However, in the following we shall employ counter terms which depend on the scalar background field. It turns out that in this case the resummation of static modes is preferred, since only for this resummation the loop expansion is an expansion in the couplings g and λ .

To leading order in the couplings, one obtains for the parameters in eq. (26) from one-loop self energy corrections [5],

$$\alpha_{01} = \frac{3}{16} g^2 + \frac{1}{2} \lambda \quad , \quad \alpha_1 = \frac{5}{6} g^2 . \quad (27)$$

The masses of the boson propagators are obtained from eqs. (1) and (26) by shifting the Higgs field σ by the average field φ (cf. (14),(15)). This yields m_L , m_T , m_σ and m_π for longitudinal and transverse part of the vector field, the Higgs field and the Goldstone boson field,

$$m_L^2 = \alpha_1 T^2 + \frac{g^2}{4} \varphi^2 \quad , \quad m_T^2 = \frac{g^2}{4} \varphi^2 \quad , \quad (28)$$

$$m_\sigma^2 = \alpha_{01} T^2 + \mu + J + 3\lambda \varphi^2 \quad , \quad m_\pi^2 = \alpha_{01} T^2 + \mu + J + \lambda \varphi^2 \quad . \quad (29)$$

The scalar masses agree with derivatives of the effective potential \tilde{V} ,

$$m_\sigma^2 = \frac{\partial^2}{\partial \varphi^2} \tilde{V}(T, \varphi; J) \quad , \quad m_\pi^2 = \frac{1}{\varphi} \frac{\partial}{\partial \varphi} \tilde{V}(T, \varphi; J) \quad , \quad (30)$$

²For a detailed discussion and references, see [5].

up to terms of higher orders in the couplings g and λ .

It has been shown that the resummed loop-expansion for the free energy is a systematic expansion in the couplings g and λ [5]. So far, however, several aspects of this resummation have remained unsatisfactory. First, higher order corrections are very important for the scalar masses³. In particular, in the Higgs phase the Goldstone boson mass m_π , as given by eq. (30), vanishes at the minimum. Hence, the expression to leading order in the couplings, given in eq. (29), is cancelled by higher order corrections. In the following we shall therefore modify the loop expansion in the Higgs phase. We replace eq. (29) by

$$m_\sigma^2 = 2\lambda\varphi^2 \quad , \quad m_\pi^2 = 0 \quad , \quad (31)$$

and we treat

$$\delta S_\beta^b = \beta \int d^3x \frac{1}{2} (\alpha_{01} T^2 + \mu + J + \lambda\varphi^2) (\sigma^2 + \pi^2) \quad , \quad (32)$$

as counter term, where σ and π again represent static modes. Note, that in the sum $\delta S_\beta^c + \delta S_\beta^b$ the temperature dependent terms cancel. Hence, we perform no thermal resummation for scalar masses in the Higgs phase.

In the symmetric phase, $\varphi = 0$, and at temperatures close to the barrier temperature $T_b = \sqrt{\mu/\alpha_{01}}$, the one-loop finite-temperature scalar masses are small, and higher order corrections are important for the Higgs boson and the Goldstone boson mass. Here, we will replace eqs. (29) by self-consistently determined scalar masses, which are defined by

$$m_\sigma^2 = m_\pi^2 = \frac{1}{\varphi} \frac{\partial}{\partial \varphi} \tilde{V}(T, 0; J) \quad . \quad (33)$$

For given vector boson masses m_L and m_T , this is a gap equation for the scalar masses, which can be solved at each order of the loop expansion.

The self-consistent scalar mass at one-loop is easily obtained from the one-loop effective potential which reads, for arbitrary resummations of the static modes,

$$\begin{aligned} \tilde{V}(T, \varphi; J) &= \frac{T^2}{6} J + \frac{1}{2} (\alpha_{01} T^2 + \mu + J) \varphi^2 + \frac{1}{4} \lambda \varphi^4 \\ &\quad - \frac{T}{12\pi} (3m_L^3 + 6m_T^3 + m_\sigma^3 + 3m_\pi^3) + \mathcal{O}(g^4, \lambda^2) \quad . \end{aligned} \quad (34)$$

From eqs. (28), (33) and (34) one obtains in the symmetric phase

$$m_\sigma^2 = m_\pi^2 = \alpha_0 T^2 + \mu + J + \mathcal{O}(g^2 m_T, \lambda m_\sigma) \quad , \quad (35)$$

³We thank P. Arnold for emphasizing this problem.

where

$$\alpha_0 = \frac{3}{16}g^2 + \frac{1}{2}\lambda - \frac{3}{16\pi}\sqrt{\frac{5}{6}}g^3 . \quad (36)$$

The corresponding counter term for perturbation theory in the symmetric phase, to be inserted in one-loop graphs in a two-loop calculation for $W(T, J)$, reads

$$\delta S_\beta^s = -\beta \int d^3x \left(\frac{1}{2}\alpha_0 T^2 (\sigma^2 + \pi^2) + \frac{1}{2}\alpha_1 T^2 W_L^2 \right) . \quad (37)$$

Having specified the vector boson and scalar masses in the Higgs phase and the symmetric phase, as given in eqs. (28), (31) and (35), the free energy can be calculated from the effective potential \tilde{V} , using the relation (17). The effective potential has two local minima,

$$\varphi_{min,1}(T, J) \equiv \varphi_s = 0 , \quad \varphi_{min,2}(T, J) \equiv \varphi_b > 0 , \quad (38)$$

which correspond to the symmetric and the Higgs phase, respectively. From eq. (34) one obtains for the free energy in both cases

$$\begin{aligned} W_s(T, J) &= \frac{T^2}{6}J - \frac{T}{3\pi}(\alpha_0 T^2 + \mu + J)^{3/2} , \\ W_b(T, J) &= \tilde{V}(T, \varphi_b(T, J); J) \\ &= \frac{T^2}{6}J + \frac{1}{2}(\alpha_{01} T^2 + \mu + J)\varphi_b^2 + \frac{1}{4}\lambda\varphi_b^4 \\ &\quad - \frac{T}{12\pi} \left(6 \left(\frac{1}{4}g^2\varphi_b^2 \right)^{3/2} + (2\lambda\varphi_b^2)^{3/2} + 3 \left(\alpha_1 T^2 + \frac{1}{4}g^2\varphi_b^2 \right)^{3/2} - 3\alpha_1^{3/2}T^3 \right). \end{aligned} \quad (39)$$

For convenience, we have subtracted the terms independent of J from W_s and W_b .

The free energy of the ground state is given by

$$W(T, 0) = \min\{W_s(T, 0), W_b(T, 0)\} . \quad (41)$$

It is a concave function, shown in fig. 1 for some choice of g and λ . The derivative of $W(T, 0)$ has a jump at the critical temperature T_c , which is characteristic for a first-order phase transition. The corresponding latent heat is given by

$$\Delta Q = T \frac{d}{dT} (W_b(T, 0) - W_s(T, 0)) |_{T=T_c} = -\mu \left(\varphi_b^2 + \frac{T_c}{\pi} (\alpha_0 T_c^2 + \mu)^{1/2} \right) , \quad (42)$$

which follows immediately from the Clausius-Clapeyron equation or, with some more work, from eqs. (39),(40). We can also consider $W(T_c, J)$, i.e., the dependence of the free energy on the external source at the critical temperature T_c . This function, shown in fig. 2, is also concave and similar to the function plotted in fig. 1. In this plot the huge linear term $T^2 J/6$, which has only the effect to shift the field square expectation value by $T^2/3$,

has been discarded in both phases. As discussed in sect. 2, the jump in the derivative at $J = 0$ yields the jump in the “order parameter” ρ at the first-order phase transition. One easily verifies that the Clausius-Clapeyron equation (25) is satisfied.

From the free energy $W(T, J)$ one can obtain the gauge invariant effective potential $V(T, \rho)$ by means of a Legendre transformation. Since the derivative of $W(T, J)$ is not continuous everywhere, one has to use the definition⁴,

$$V(T, \rho) = \sup_J \{W(T, J) - \frac{1}{2}\rho J\} . \quad (43)$$

This yields the convex, non-analytic function, plotted in fig. 3 as full line. One may also compute the ordinary Legendre transform $V_s(T, \rho)$ and $V_b(T, \rho)$ of $W_s(T, J)$ and $W_b(T, J)$, respectively. Neglecting constant terms this yields

$$\begin{aligned} V_s(T, \rho) &= \frac{1}{2}(\alpha_0 T^2 + \mu)\rho' - \frac{\pi^2}{6T^2}\rho'^3 , \\ V_b(T, \rho) &= \tilde{V}(T, \sqrt{\rho'}, 0) , \end{aligned} \quad (44)$$

where we have used

$$\frac{1}{2}\rho' \equiv \frac{1}{2} \left(\rho - \frac{T^2}{3} \right) = \frac{\partial W_b(T, J)}{\partial J} - \frac{T^2}{6} = \frac{1}{2}\varphi_b^2 + \left. \frac{\partial \tilde{V}}{\partial \varphi} \right|_{\varphi_b} \frac{\partial \varphi_b}{\partial J} = \frac{1}{2}\varphi_b^2 . \quad (45)$$

V_s and V_b are also shown in fig. 3. In the region outside of the two local minima, V_s and V_b , respectively, coincide with the convex effective potential $V(T, \rho)$. Between the two local minima, V_s and V_b represent two analytical continuations of $V(T, \rho)$, which meet at the “matching point” $\rho_M = T^2/3$. At this point, marked by a cross in the plot, the first derivatives of both curves coincide.

The non-convex “effective potential” obtained by combining V_s and V_b on both sides of the “matching point” is almost identical with the gauge invariant “effective potential” obtained in [18]. If the root appearing in $V_b(T, \rho)$ is expanded to order ρ^2/T^4 , which corresponds to the reduction to the three-dimensional theory considered in [18], both “effective potentials” are identical. The generation of a barrier between two local minima as analytic continuation from a convex effective potential is reminiscent of the treatment of first-order phase transitions in condensed matter physics [26]. However, the precise physical meaning of the resulting non-convex “effective potential” still remains to be understood.

In [18] it was pointed out that the usual Landau-gauge effective potential and the gauge invariant effective potential lead to different predictions for observables like latent

⁴For a discussion and references, see [22].

heat, critical temperature etc. Our derivation of the gauge invariant effective potential in this section demonstrates that these differences are a consequence of different choices of the resummation procedure. Based on the arguments given above, the asymmetric resummation which treats symmetric phase and Higgs phase differently, appears better justified.

The results of [18] were obtained by performing an expansion around the tree-level minima in the Higgs phase and in the symmetric phase. This approach has been considered at two-loop level [25, 27], and some problems have been discussed by Laine [27]. In this section we have reproduced the results of [18] by expanding around local minima of the effective potential \tilde{V} which includes quantum corrections. As we shall demonstrate in the following section, this procedure can be extended to two loops. At this level the fundamental infrared problem of the symmetric phase will also become apparent, and we shall discuss under which conditions the loop expansion can yield a good approximation of thermodynamic quantities relevant for the electroweak phase transition.

5 Two-loop results

In this section we shall extend the asymmetric resummation to two loops in order to examine the convergence of the perturbative expansion. In recent years several two-loop calculations have already been carried out. In [4] all two-loop contributions involving only the gauge coupling were evaluated, which yield the effective potential \tilde{V} to order g^4, λ . In this calculation scalar masses were set equal to zero. A complete two-loop calculation of \tilde{V} to order g^4, λ^2 , including scalar loops, has been carried out in [7], where also the full standard model has been considered. Here the masses (28),(29), with $J = 0$, were used in the symmetric phase and the Higgs phase. The same result has also been obtained by using as intermediate step the effective three-dimensional theory, which is obtained by integrating out modes with non-zero Matsubara frequencies [28]. Furthermore, the effective potential of the three-dimensional theory has been evaluated in general covariant [29] and 't Hooft background gauges [30].

In all these calculations the resummation of scalar masses has been performed in the same way in the symmetric and the Higgs phase. However, on physical grounds, as explained in the previous section, an asymmetric treatment of the two phases appears more appropriate. In the Higgs phase scalar masses are given by eq. (31) and the counter term is defined by the sum $\delta S_\beta^c + \delta S_\beta^b$, as discussed in sect. 4. In the symmetric phase

the scalar masses are self-consistently determined from eq. (33),

$$m_\sigma^2 = m_\pi^2 = \frac{1}{\varphi} \frac{\partial}{\partial \varphi} \tilde{V}(T, 0; J) , \quad (46)$$

where the potential \tilde{V} is calculated with the counter term δS_β^s given in eq. (37). Note, that in the two-loop calculation the counter term to be inserted in the one-loop graph is $\mathcal{O}(g^3)$, whereas the scalar mass determined from eq. (33) is of higher order in g .

The two-loop potential \tilde{V} for arbitrary masses m_σ and m_π can be extracted from [4, 7]. We have listed the individual contributions corresponding to the graphs of fig. 9 in the appendix, omitting terms independent of φ and terms which cancel in the sum. The two-loop potential contains terms linear in m_σ and m_π . In the symmetric phase, where the counter term is given by (37), these terms cancel in the sum. In the Higgs phase they contribute to the potential.

In the symmetric phase the scalar masses are determined self-consistently by eq. (33). With $m_T = g\varphi/2$, the two-loop potential yields a contribution which diverges logarithmically at $\varphi \approx 0$ (cf. (56)),

$$m_\sigma^2 \approx -\frac{33g^4}{128\pi^2} T^2 \ln \beta m_T . \quad (47)$$

Following [5] we regularize this divergence by means of a ‘‘magnetic mass’’ term. In eq. (47) we substitute $m_T^2 = g^2\varphi^2/4 + \gamma^2 g^4 T^2/(9\pi^2)$. In the following we shall use $\gamma = 1$, which follows from one-loop gap equations [5, 6]. We have checked that the results of our numerical analysis change only insignificantly if we vary the parameter γ between 0.3 and 3.0. The deviation of the most sensitive quantity $\Delta Q/T_c^4$ from the plotted $\gamma = 1$ result is invisible for small Higgs mass and increases up to 8% at $m_H = 70$ GeV. Eq. (33) for the scalar masses can be solved iteratively. In the first step one inserts in the two-loop potential \tilde{V} the one-loop scalar masses (28). The mass m_σ obtained in this first step of iteration is already a very good approximation to the exact solution in the range of Higgs masses which we shall consider.

Given the two-loop potential in the symmetric phase and the Higgs phase, we can numerically determine the critical temperature T_c , where the two potentials at their respective local minima are degenerate. Differentiation with respect to temperature and the external source J then yields latent heat and jump in the order parameter $\rho = 2\Phi^\dagger\Phi$. The results are shown in figs. 4 - 6, assuming standard model values $m_W = 80.22$ GeV and $v = 251.78$ GeV at zero temperature.

In fig. 4 the critical temperature in units of the Higgs mass is plotted as function of the Higgs mass in the range $30 \text{ GeV} < m_H < 80 \text{ GeV}$. Below 30 GeV the high-temperature

expansion is unreliable, and above 80 GeV the convergence of the loop expansion deteriorates rapidly. The two-loop results are compared with one-loop results for the “old resummation” [7] and for the “new resummation” described above. In the “new resummation” the one-loop result is lowered whereas the two-loop result is increased, improving the convergence of the loop expansion considerably. The relative change of an observable from one-loop to two-loop may be characterized by $\delta = 2|O_1 - O_2|/(O_1 + O_2)$. In the “new resummation” $\delta \sim 0.04$ in the whole range of Higgs masses considered.

The jump in the order parameter at the critical temperature T_c is shown in fig. 5. In the case of “old resummation” φ_c corresponds to the position of the second minimum, for “new resummation” it is $\sqrt{\Delta\rho}$. Again the “new resummation” procedure improves the convergence significantly. The relative error increases from $\delta \sim 0.01$ at $m_H = 40$ GeV to $\delta \sim 0.2$ at $m_H = 70$ GeV.

In fig. 6 the latent heat ΔQ in units of the critical temperature is plotted as function of the Higgs mass. This is a measure of the strength of the first-order phase transition. Like the jump in the order parameter it decreases with increasing Higgs mass. Based on the Clausius-Clapeyron equation, which is satisfied exactly, we expect $\Delta Q \sim \Delta\rho$. Hence, the convergence should be worse than for the order parameter. This is indeed the case. The relative error increases from $\delta \sim 0.1$ at $m_H = 40$ GeV to $\delta \sim 0.4$ at $m_H = 70$ GeV.

It appears satisfactory that the new, asymmetric resummation procedure leads to an improved convergence of the perturbative expansion. The “old resummation” is based on a systematic expansion of the free energy in powers of the couplings g and λ . Therefore in the symmetric phase, where the scalar masses are positive, the differences can only correspond to contributions of higher order. This ambiguity in the resummation procedure is analogous to the well known dependence of results in perturbative QCD on the renormalization scheme. However, setting the Goldstone mass to zero in the Higgs phase does not correspond to a simple rearrangement of the series, since terms non-analytic in m_π are present. The correct treatment of the Higgs phase is the main qualitative advantage of the new resummation.

6 Comparison with lattice simulations

In the previous sections we have presented a quantitative description of the electroweak phase transition in the perturbative approach. Using different resummations in the Higgs phase and in the symmetric phase, we concluded that for Higgs boson masses below

~ 70 GeV the perturbative approach converges, and that this description is therefore self-consistent. However, for Higgs masses above the present experimental lower bound, $m_H > 63$ GeV, the loop expansion becomes unreliable. In this relevant range of the parameter space the electroweak phase transition can only be understood by means of non-perturbative methods. Lattice Monte Carlo simulations provide a well defined and systematic approach to study this problem. For all Higgs masses, non-perturbative effects may be important in the symmetric phase. By comparing data from lattice simulations for the SU(2) Higgs model with the perturbative results one can hope to identify non-perturbative features and to achieve a better understanding of the electroweak phase transition. Therefore, in this section we shall present a detailed comparison between data of the recent large scale four-dimensional lattice works [10, 11] and published results of the “old resummation” [7]. For the considered Higgs masses they differ little from the “new resummation” results.

Monte Carlo simulations for Higgs boson masses near or above the W-boson mass are technically difficult, thus in [10, 11] the Higgs masses $m_H \approx 18$ GeV and $m_H \approx 49$ GeV have been studied. Since in this parameter range the perturbative expansion converges rather well, one may expect agreement between perturbative and non-perturbative results with comparable accuracy.

The $g^3, \lambda^{3/2}$ -potential of [7] involves a high-temperature expansion up to order $(m/T)^3$, which is unsatisfactory for $m_H \approx 18$ GeV. Thus, we have included all one-loop contributions of order $(m/T)^4$ in our present $g^3, \lambda^{3/2}$ -potential. Note, that the numerical evaluation of the one-loop temperature integrals gives a result which agrees with the above approximation up to a few percent.

For small Higgs boson masses the renormalization scheme dependence is non-negligible. Therefore, instead of the $\overline{\text{MS}}$ -scheme with $\bar{\mu} = T$, we shall use the scheme suggested by Arnold and Espinosa [4], which includes the most important zero-temperature renormalization effects. In this scheme the correction to the $\overline{\text{MS}}$ -potential, used for both the one- and the two-loop results, reads

$$\delta V = \frac{\varphi^2}{2} \left(\delta\mu + \frac{1}{2\beta^2} \delta\lambda \right) + \frac{\delta\lambda}{4} \varphi^4, \quad (48)$$

where

$$\delta\mu = \frac{9g^4 v^2}{256\pi^2}, \quad \delta\lambda = -\frac{9g^4}{256\pi^2} \left(\ln \frac{m_W^2}{\bar{\mu}^2} + \frac{2}{3} \right). \quad (49)$$

Here v is the zero-temperature vacuum expectation value and m_W is the W-boson mass at $T = 0$.

In [11] several observables have been determined, including renormalized masses at zero temperature (m_H , m_W), critical temperature (T_c), jump in the order parameter (φ_c), latent heat (ΔQ) and surface tension (σ). As usual, the dimensionful quantities have been normalized by the proper power of the critical temperature. The simulations have been performed on $L_t = 2$ and $L_t = 3$ lattices (L_t is the temporal extension of the finite-temperature asymmetric lattice). The $L_t = 3$ results should be closer to the continuum values, and we therefore compare these data with the perturbative results. An exception is the surface tension for which only $L_t = 2$ data exist.

In the previous sections we have only evaluated T_c , φ_c and ΔQ , which follow from the free energy of a homogeneous phase. The surface tension is more complicated to calculate, since it involves the boundary between two phases. In perturbation theory this is related to the effective potential \tilde{V} in the region between the two local minima. For completeness, we include the surface tension in the comparison, although so far no satisfactory treatment has been achieved in perturbation theory for Higgs masses above ~ 40 GeV.

The statistical errors of these observables are normally determined by comparing statistically independent samples. The systematic errors can be estimated by the difference between the $L_t = 2$ and the $L_t = 3$ data. As fig. 15 of [11] suggests, the true systematic error for T_c/m_H may be larger than this naive estimate. Thus, for T_c/m_H we have doubled the above error. For the surface tension, where only $L_t = 2$ data exist, the systematic error has been estimated as twice the statistical one. A correct comparison has to include errors on the parameters used in the perturbative calculation. These uncertainties are connected with the fact that neither the Higgs boson mass nor the gauge coupling has been determined exactly. Therefore, the perturbative prediction for an observable is not one definite value but rather an interval, given by the uncertainties of m_H and g . In this analysis only the statistical errors in the determination of the Higgs boson mass and the gauge coupling have been included. We have also neglected corrections due

	$m_H \approx 18$ GeV	$m_H \approx 49$ GeV
ΔQ from Clausius-Clapeyron eq.	.0236(14)	.00171(15)
direct lattice result for ΔQ	.0194(15)	.00151(12)

Table 1: Comparison of the latent heat in lattice units obtained by using the Clausius-Clapeyron equation and lattice Monte Carlo simulations. The data are from ref. [11].

to the different renormalization conditions used for the gauge coupling g and the order parameter $\Phi^\dagger\Phi$ on the lattice and in the continuum. These corrections are expected to be of relative order g^2 .

Let us first check the validity of the Clausius-Clapeyron equation for the lattice Monte Carlo simulations. The first line of table 1 contains ΔQ obtained by eq. (25) from lattice results for $\Delta\rho$ and m_H^2 . The second line contains the latent heat determined directly by lattice simulations. As usual, the numbers in the parentheses denote the statistical errors. The values for $m_H \approx 49$ GeV agree within one standard deviation. For $m_H \approx 18$ GeV, however, there is a small discrepancy.

The comparison for φ_c/T_c , $\Delta Q/T_c^4$, σ/T_c^3 and T_c/m_H is shown in fig. 7 ($m_H \approx 18$ GeV) and in fig. 8 ($m_H \approx 49$ GeV). The dots with error bars represent the perturbative result at one-loop (g^3) and at two-loop (g^4) level. For each quantity the dashed lines show the region allowed by the statistical error, whereas the dotted lines include the systematic error as well. Note, that the values of g and m_H/m_W are those of [11]. We emphasize that, both in the perturbative calculation and in the lattice simulations, the surface tension is the most problematic quantity.

For $m_H \approx 18$ GeV (cf. fig. 7) both the one-loop and the two-loop results are in good agreement with the lattice data. For $m_H \approx 49$ GeV (cf. fig. 8) the two-loop results agree definitely better with the Monte Carlo data, except for the surface tension. The two plots may be interpreted in the following way. For small Higgs boson masses the perturbative approach is in very good shape, already the one-loop approximation gives a reliable result. As m_H grows, the higher order contributions become more and more important, yet a two-loop calculation is still satisfactory for $m_H \approx 49$ GeV. In this range of parameters the non-perturbative features of the symmetric phase are not important enough to destroy the perturbative picture.

7 Conclusions

In the present paper a quantitative description of the electroweak phase transition based on a gauge invariantly coupled source term has been attempted. Our main result is that for Higgs masses below ~ 70 GeV thermodynamic observables can be evaluated with reasonable accuracy in perturbation theory. Above $m_H \sim 70$ GeV the perturbative expansion breaks down, which is in agreement with previous estimates [5].

The main technical achievement is the realization of different resummation proce-

dures in the symmetric phase and in the Higgs phase, which are expected to improve the convergence of perturbation theory. Such an improvement has been explicitly verified for the available terms up to two-loop order. Due to infrared divergencies of the non-abelian theory a cutoff is needed in the symmetric phase at two-loop order. We emphasize that due to the small cutoff dependence at not too large Higgs masses perturbation theory may work with some accuracy in the symmetric phase. The size of non-perturbative effects can only be determined by comparing perturbative results with fully non-perturbative lattice simulations.

We have carried out such a comparison, based on results of recent simulations on large lattices [11]. The good quantitative agreement found for Higgs mass values $m_H \approx 18$ GeV and $m_H \approx 49$ GeV is interpreted as evidence for the correctness of the present understanding of the electroweak phase transition. Non-perturbative effects present in the symmetric phase are neglected by perturbation theory, but they should contribute to the lattice results. We conclude that these effects can not be of major importance at small Higgs mass, since otherwise no quantitative agreement with lattice data could be observed.

Applying the Clausius-Clapeyron equation to the electroweak phase transition a simple relation between latent heat and jump of the order parameter has been derived. Being in good agreement with perturbative as well as with lattice data, it strengthens confidence in the correctness of the treatment of the phase transition.

The above arguments support the conclusion that our understanding of the electroweak phase transition has reached a quantitative level for Higgs masses up to ~ 70 GeV. A strong decrease of the strength of the first-order transition with increasing Higgs mass is observed. However, a complete understanding of the process of symmetry restoration for large Higgs masses is still lacking. Other important questions include the description of metastable and unstable states, relevant for the dynamics of the transition.

8 Appendix

In this appendix, for the convenience of the reader, all the contributions to the effective potential from one and two-loop graphs (see fig. 9) are listed in $\overline{\text{MS}}$ -scheme. This calculation has already been performed in [4] up to order g^4 and extended in [7, 28] to the order g^4, λ^2 . The different contributions are presented according to the counterterm method of resummation, applied to the zero modes only [4]. The scalar resummation

is left unspecified, since it is different in the symmetric phase and in the Higgs phase following the approach of section 5. It is characterized by the values of the scalar masses m_σ and m_π , and the scalar counter term C_s , present in V_a .

Tree level potential and one-loop corrections are collected in V_1 while the two-loop contributions $V_a \dots V_k$ are labelled in correspondence with the diagrams of fig. 9. Linear mass terms, poles in ϵ and terms proportional to ι_ϵ (see ref. [4]), which cancel systematically in the final result, are not shown and the limit $\epsilon \rightarrow 0$ has already been performed. This is the reason for the vanishing of V_b , which would only contribute to the well known cancellation of linear mass terms of order g^3 .

$$V_1 = \frac{\varphi^2}{2} \left[\mu + \frac{1}{\beta^2} \left(\frac{1}{2} \lambda + \frac{3}{16} g^2 \right) \right] + \frac{\lambda}{4} \varphi^4 - \frac{1}{12\pi\beta} \left[m_\sigma^3 + 3 m_\pi^3 + 6 m^3 + 3 m_L^3 \right] \quad (50)$$

$$- \frac{1}{64\pi^2} \left\{ (12\lambda^2 \varphi^4 + 12\lambda\mu\varphi^2 + 9m^4) \left(\ln \bar{\mu}^2 \beta^2 - c_1 + \frac{3}{2} \right) - 6m^4 - \frac{59}{12\beta^2} g^2 m^2 \right\}$$

$$V_a = \frac{1}{8\pi\beta} (m_\sigma + 3m_\pi) C_s \quad , \quad V_b = 0 \quad (51)$$

$$V_c = \frac{\lambda}{\beta^2} \left[-\frac{m_\sigma + 3m_\pi}{16\pi\beta} + \frac{1}{64\pi^2} \left\{ 3m_\sigma^2 + 6m_\sigma m_\pi + 15m_\pi^2 - 6\lambda\varphi^2 \left(\ln \bar{\mu}^2 \beta^2 - c_1 + \frac{3}{2} \right) \right\} \right] \quad (52)$$

$$V_d = \frac{3g^2}{128\beta^2} \left[-\frac{m_\sigma + 3m_\pi}{\pi\beta} \right. \quad (53)$$

$$\left. + \frac{1}{\pi^2} \left\{ (m_\sigma + 3m_\pi)(2m + m_L) - \frac{1}{4} (4m^2 + 6\lambda\varphi^2) \left(\ln \bar{\mu}^2 \beta^2 - c_1 + \frac{5}{6} \right) \right\} \right]$$

$$V_e = \frac{3g^2}{256\pi^2\beta^2} \left[32m_L m - 9m^2 \left(\ln \bar{\mu}^2 \beta^2 - c_1 - \frac{125}{54} \right) \right] \quad (54)$$

$$V_f = \frac{3g^2}{128\pi^2\beta^2} \left[2m^2 \left(\ln \frac{\beta}{3} - \frac{1}{12} \ln \bar{\mu}^2 \beta^2 - \frac{1}{6} c_1 + \frac{1}{4} c_2 + \frac{1}{4} \right) + m_\pi (m_\sigma + m_\pi) \right] \quad (55)$$

$$\begin{aligned}
& +\frac{1}{2} \left(m_\sigma^2 + 3m_\pi^2 \right) \left(-4 \ln \frac{\beta}{3} + \ln \bar{\mu}^2 \beta^2 - c_2 \right) - \frac{1}{m} (m_\sigma - m_\pi)^2 (m_\sigma + m_\pi) - m (m_\sigma + 3m_\pi) \\
& - \frac{1}{m^2} \left(m_\sigma^2 - m_\pi^2 \right)^2 \ln (m_\sigma + m_\pi) + \left(m^2 - 4m_\pi^2 \right) \ln (2m_\pi + m) \\
& + \frac{1}{m^2} \left\{ m^4 - 2 \left(m_\sigma^2 + m_\pi^2 \right) m^2 + \left(m_\sigma^2 - m_\pi^2 \right)^2 \right\} \ln (m_\sigma + m_\pi + m) \Big]
\end{aligned}$$

$$\begin{aligned}
V_{gh} = & \frac{g^2}{16\pi^2\beta^2} \left[\frac{m^2}{8} \left(31 \ln \bar{\mu}^2 \beta^2 - 66 \ln m + 39 \ln 3 - \frac{11}{2} c_1 - \frac{51}{2} c_2 - \frac{145}{4} - 102 \ln \beta \right) \right. \\
& \left. - 3m_L m + \frac{3}{2} m_L^2 + \left(\frac{3}{2} m^2 - 6m_L^2 \right) \ln (2m_L + m) \right] \quad (56)
\end{aligned}$$

$$V_j = -\frac{3\lambda^2\varphi^2}{32\pi^2\beta^2} \left[\ln \frac{9\bar{\mu}^2}{\beta^2} - c_2 - 2 \ln \{ m_\sigma (m_\sigma + 2m_\pi) \} \right] \quad (57)$$

$$\begin{aligned}
V_k = & \frac{3g^2}{64\pi^2\beta^2} \left[m^2 \left(\frac{5}{4} \ln \frac{\beta}{9\bar{\mu}} + \frac{5}{8} c_2 + \ln (2m_L + m_\sigma) \right) + \frac{m_\sigma^4}{4m^2} \ln m_\sigma + \frac{1}{2} m_\sigma m \right. \\
& \left. - \frac{1}{2m^2} (m^2 - m_\sigma^2)^2 \ln (m + m_\sigma) + \left(2m^2 - m_\sigma^2 + \frac{m_\sigma^4}{4m^2} \right) \ln (2m + m_\sigma) + \frac{1}{4} m_\sigma^2 \right]. \quad (58)
\end{aligned}$$

Here evaluating the scalar one- and two-loop temperature integrals the constants

$$c_1 \approx 5.4076 \quad \text{and} \quad c_2 \approx 3.3025 \quad (59)$$

have been introduced following [31] and [32, 33], respectively.

References

- [1] D. A. Kirzhnits, JETP Lett. 15 (1972) 529;
D. A. Kirzhnits and A. D. Linde, Phys. Lett. B42 (1972) 471
- [2] V. A. Kuzmin, V. A. Rubakov and M. E. Shaposhnikov, Phys. Lett. B155 (1985) 36
- [3] M. Dine, R. G. Leigh, P. Huet, A. Linde and D. Linde, Phys. Rev. D46 (1992) 550
- [4] P. Arnold and O. Espinosa, Phys. Rev. D47 (1993) 3546
- [5] W. Buchmüller, Z. Fodor, T. Helbig and D. Walliser, Ann. Phys. 234 (1994) 260
- [6] J. R. Espinosa, M. Quirós and F. Zwirner, Phys. Lett. B314 (1993) 206
- [7] Z. Fodor and A. Hebecker, Nucl. Phys. B432 (1994) 127
- [8] B. Bunk, E.-M. Ilgenfritz, J. Kripfganz and A. Schiller, Nucl. Phys. B403 (1993) 453
- [9] K. Kajantie, K. Rummukainen and M. Shaposhnikov, Nucl. Phys. B407 (1993) 356;
K. Farakos, K. Kajantie, K. Rummukainen and M. E. Shaposhnikov, Phys. Lett. B 336 (1994) 494
- [10] F. Csikor, Z. Fodor, J. Hein, K. Jansen, A. Jaster and I. Montvay, Phys. Lett. B334 (1994) 405
- [11] Z. Fodor, J. Hein, K. Jansen, A. Jaster and I. Montvay, preprint DESY 94-159, to appear in Nucl. Phys. B
- [12] F. Karsch, T. Neuhaus and A. Patkós, preprint BI-TP 94/27 (1994)
- [13] H. G. Evertz, J. Jersák and K. Kanaya, Nucl. Phys. B285 (1987) 229
- [14] M. Reuter and C. Wetterich, Nucl. Phys. B408 (1993) 91
- [15] W. Buchmüller and O. Philipsen, preprint DESY 94-202 (1994)
- [16] K. Jansen, J. Jersák, C.B. Lang, T. Neuhaus and G. Vones, Phys. Lett. B155 (1985) 268
- [17] M. Lüscher, unpublished notes (1988)

- [18] W. Buchmüller, Z. Fodor and A. Hebecker, Phys. Lett. B331 (1994) 131
- [19] J.I. Kapusta, *Finite-temperature field theory* (Cambridge Univ. Press, 1989)
- [20] J. Zinn-Justin, *Quantum Field Theory and Critical Phenomena* (Clarendon Press, Oxford, 1993) pp. 242–243
- [21] R. Fukuda and E. Kyriakopoulos, Nucl. Phys. B85 (1975) 354
- [22] L. O’Raifeartaigh, A. Wipf and H. Yoneyama, Nucl. Phys. B271 (1986) 653
- [23] N.K. Nielsen, Nucl. Phys. B101 (1975) 173;
R. Fukuda and T. Kugo, Phys. Rev. D13 (1976) 3469
- [24] H. B. Callan, *Thermodynamics* (Wiley, New York, 1960)
- [25] K. Farakos, K. Kajantie, K. Rummukainen and M. Shaposhnikov, preprint CERN-TH 7220/94 (1994)
- [26] J.S. Langer, Physica A73 (1974) 61
- [27] M. Laine, preprint HU-TFT-94-46 (1994)
- [28] K. Farakos, K. Kajantie, K. Rummukainen and M. Shaposhnikov, Nucl. Phys. B425 (1994) 67
- [29] M. Laine, Phys. Lett. B335 (1994) 173
- [30] J. Kripfganz, A. Laser and M.G. Schmidt, preprint HD-THEP-95-1 (1995)
- [31] L. Dolan and R. Jackiw, Phys. Rev. D9 (1974) 3320
- [32] R.R. Parwani, Phys. Rev. D45 (1992) 4695
- [33] P. Arnold and C. Zhai, preprint UW/PT-94-03 (1994)

Figure captions

Fig.1 Free energy at zero source term as a function of the temperature ($m_H = 70$ GeV).

Fig.2 Free energy at the critical temperature as a function of the source J ($m_H = 70$ GeV).

Fig.3 Gauge invariant effective potential (solid line) and its analytic continuations from the single phase regions into the mixed phase region (dashed line). The cross denotes the matching point.

Fig.4 Ratio of critical temperature and zero-temperature Higgs mass as a function of the Higgs mass.

Fig.5 Square root of the jump of the order parameter $\varphi_c = \sqrt{\Delta\rho}$ in units of the critical temperature T_c .

Fig.6 Higgs mass dependence of the latent heat ΔQ of the phase transition.

Fig.7 Comparison of the lattice data with the one-loop and two-loop perturbative results for $m_H \approx 18$ GeV.

Fig.8 Comparison of the lattice data with the one-loop and two-loop perturbative results for $m_H \approx 49$ GeV.

Fig.9 Two-loop diagrams contributing to the effective potential.

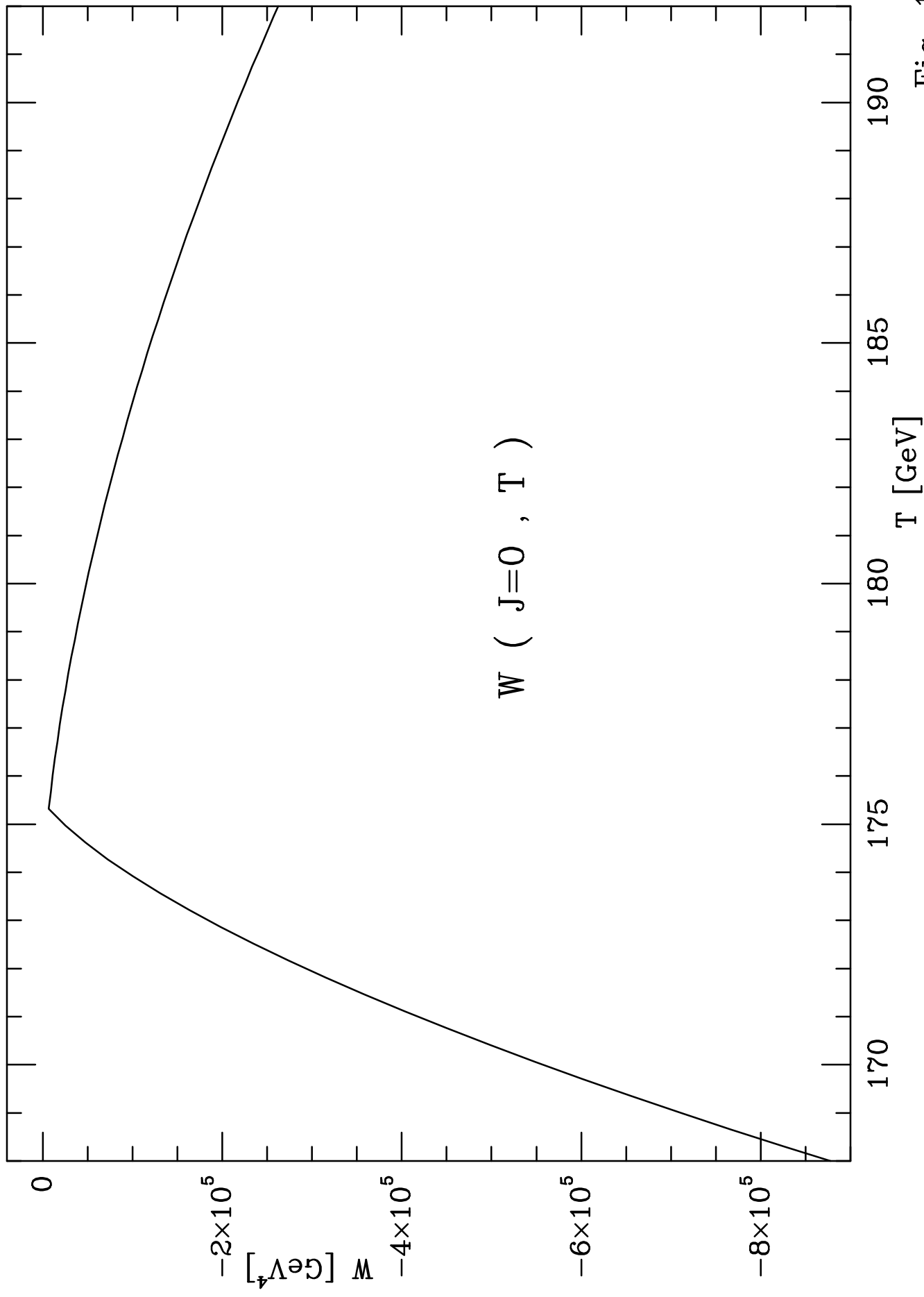


Fig. 1

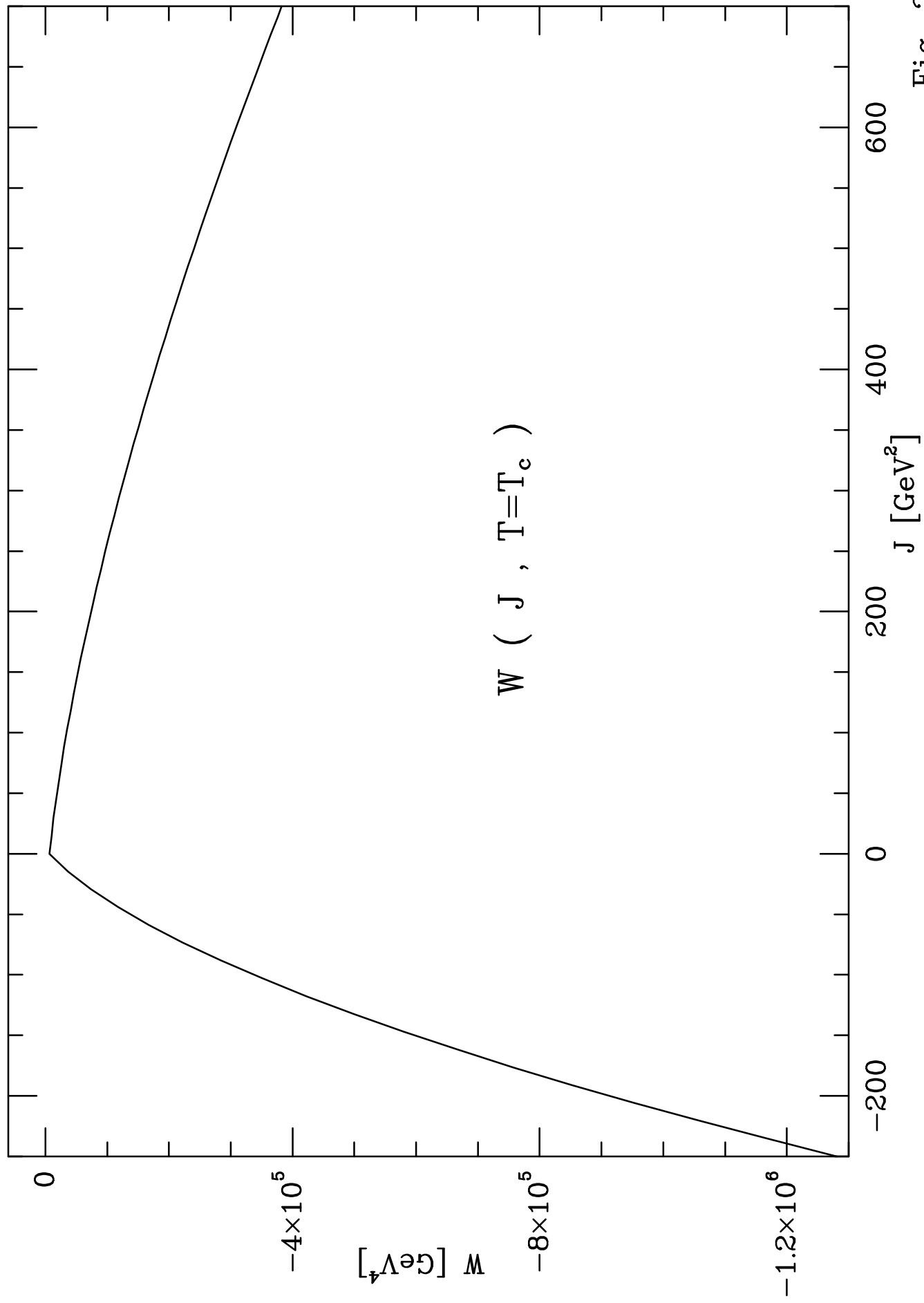


Fig. 2

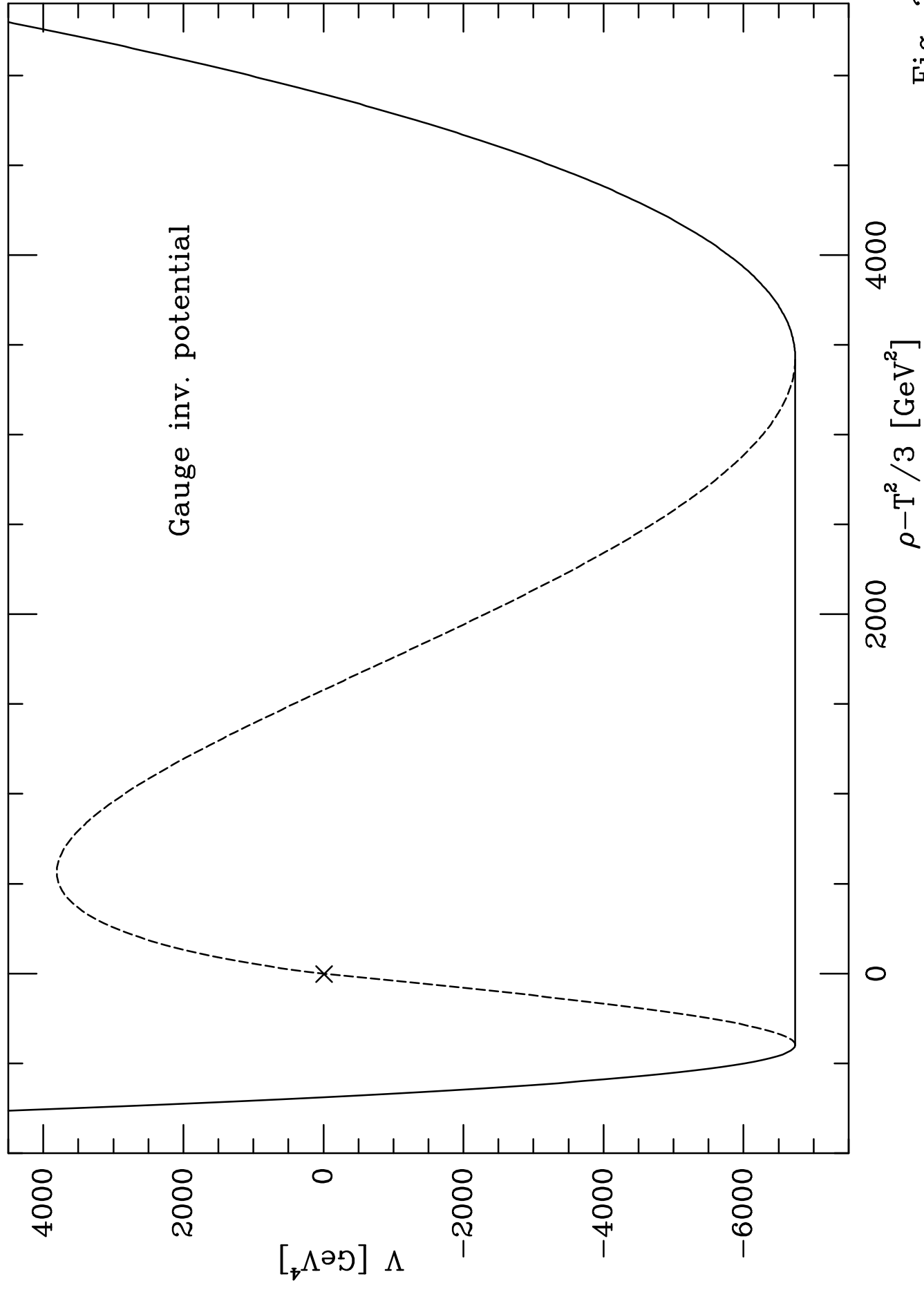


Fig. 3

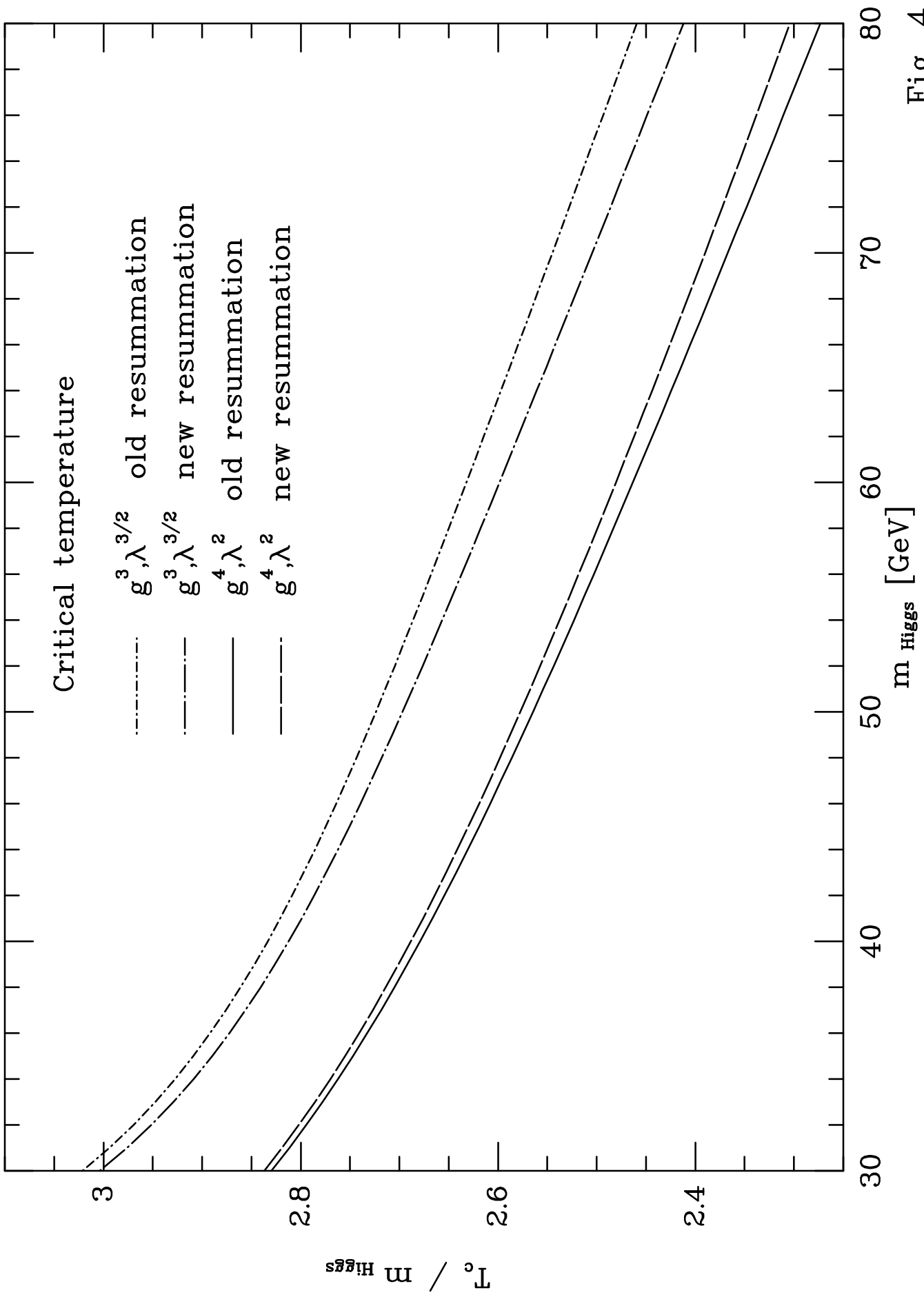


Fig. 4

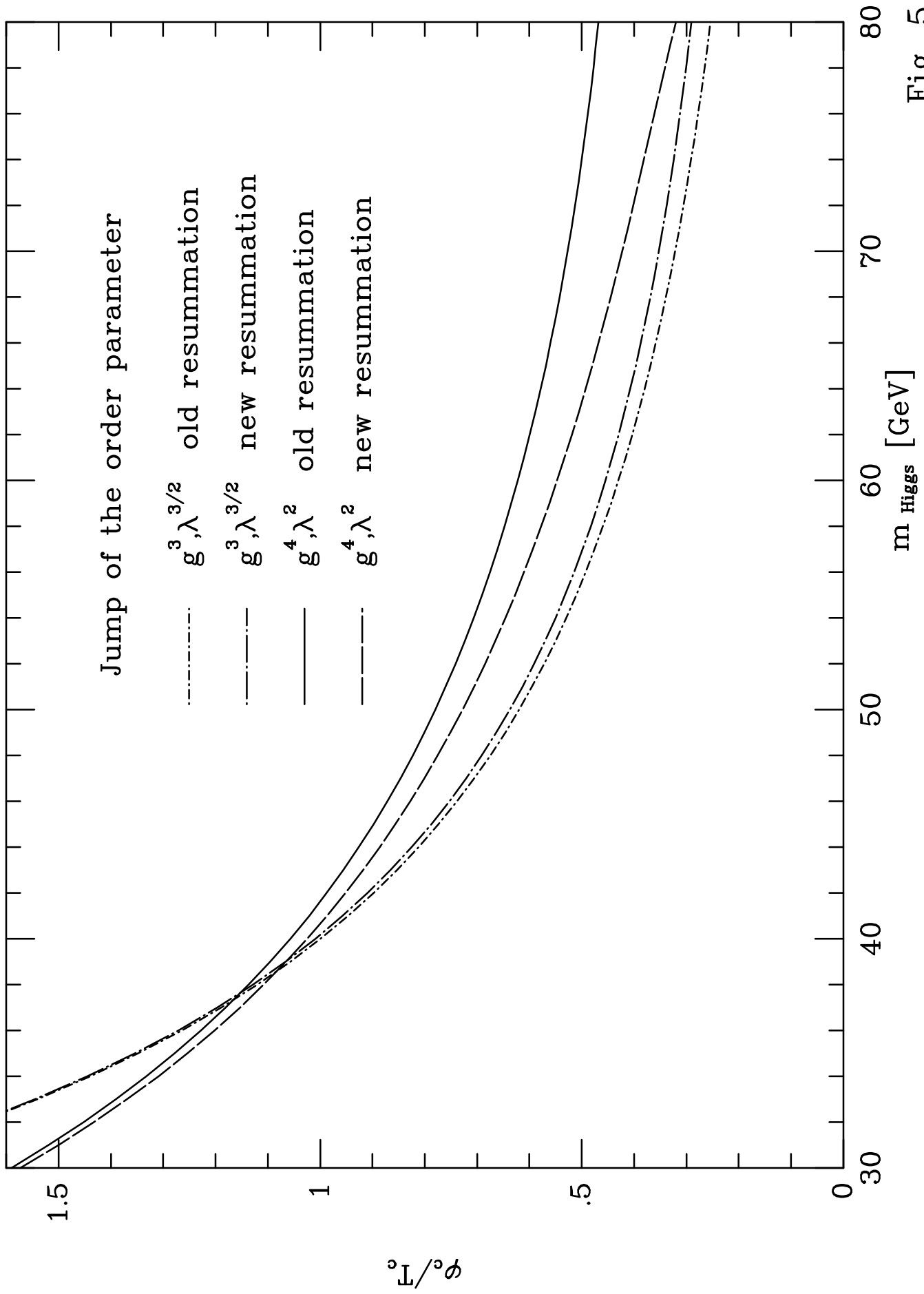


Fig. 5

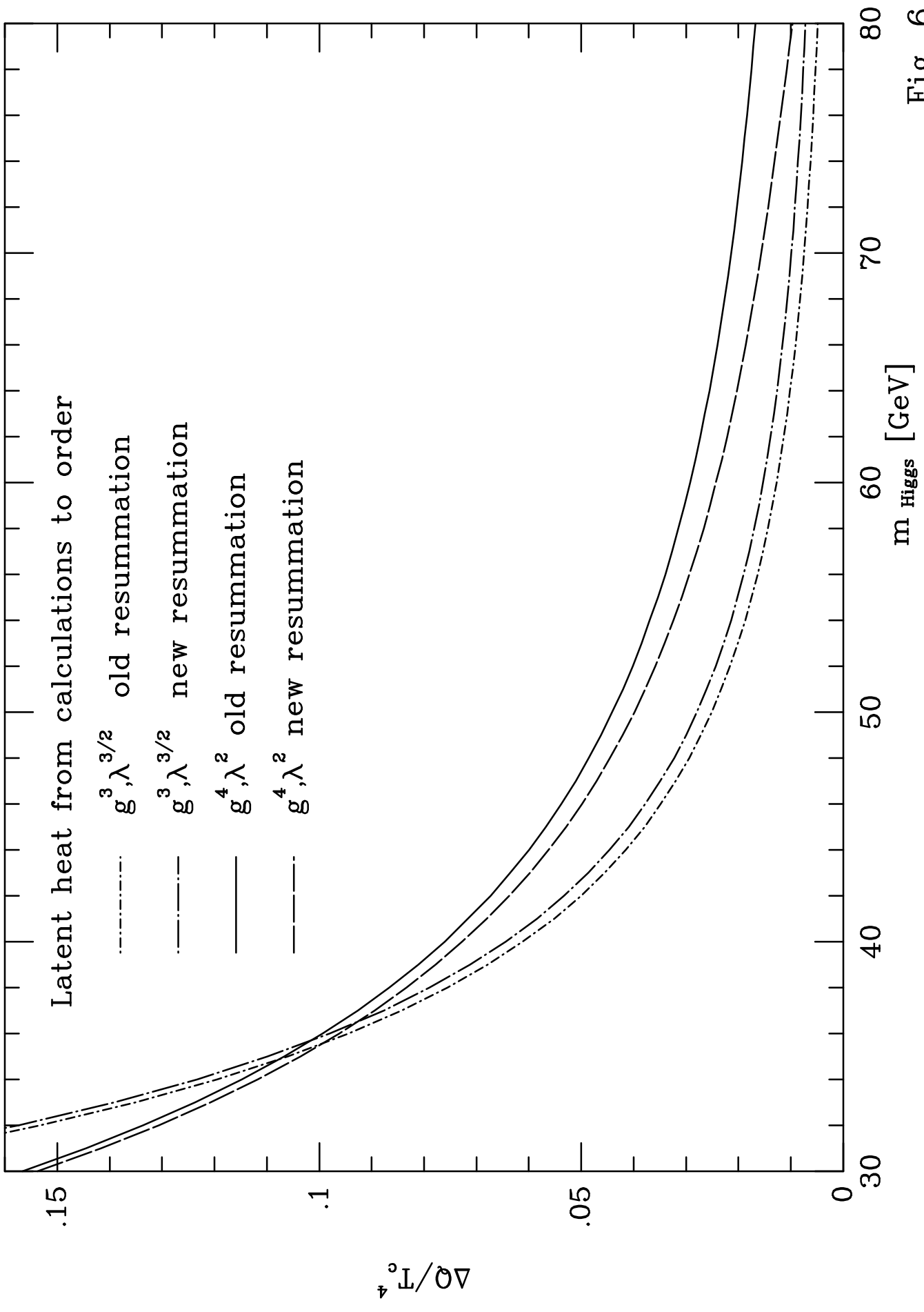


Fig. 6

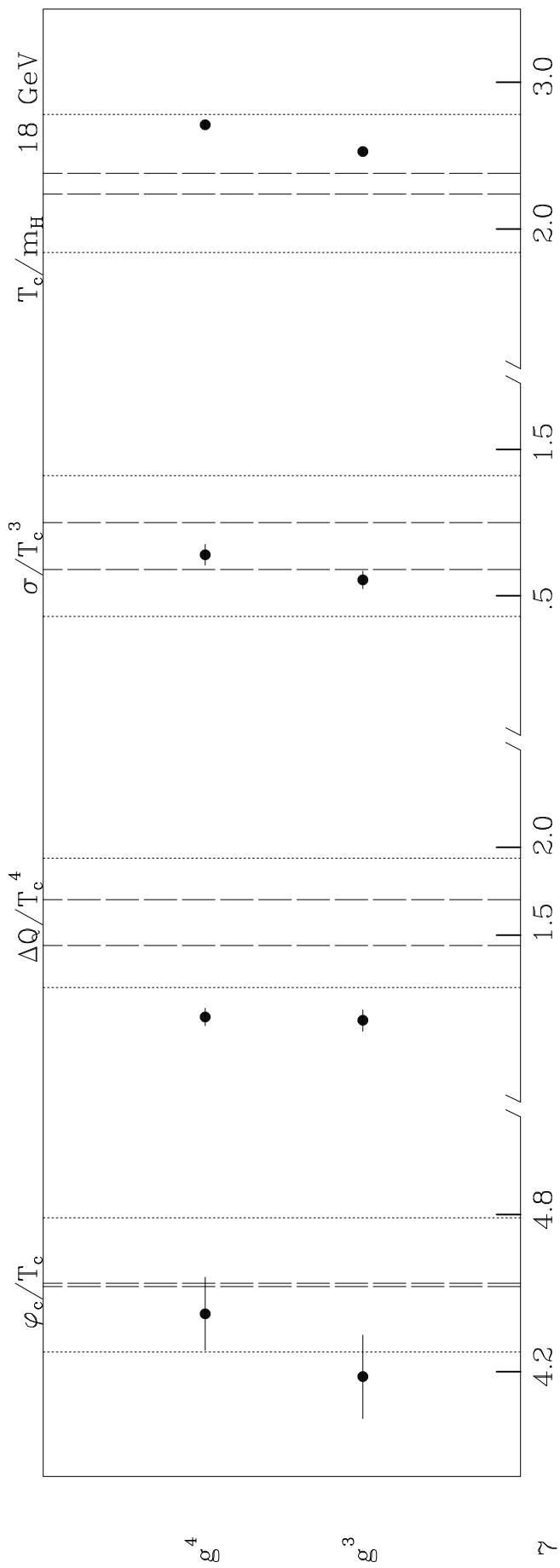


Fig. 7

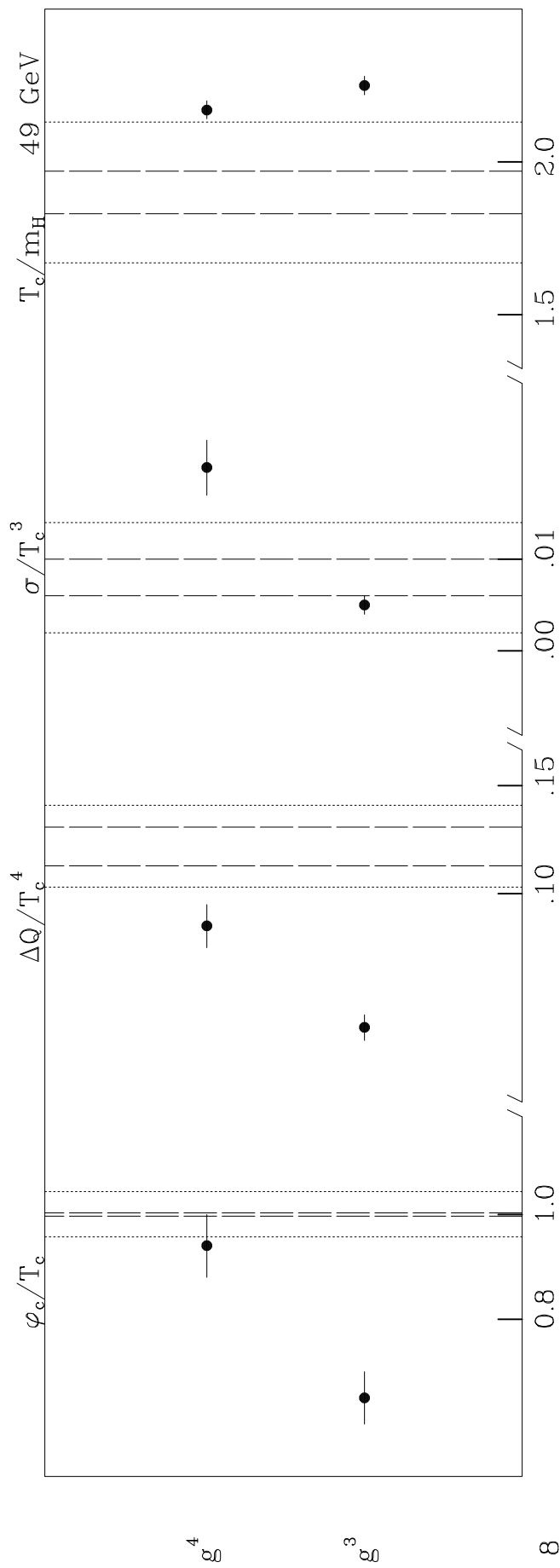


Fig. 8

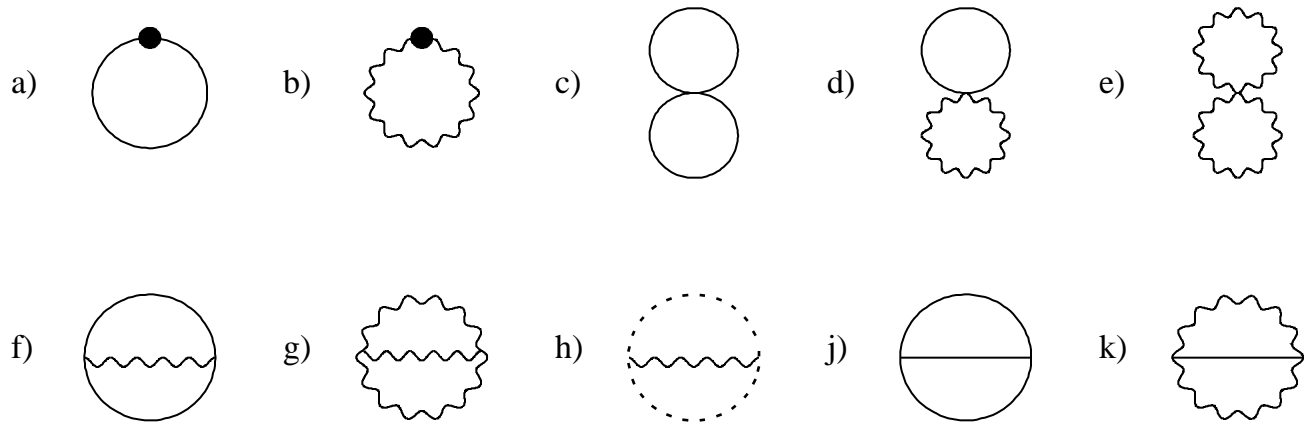


Fig. 9